SCIENTIFIC PAPER
Published: December 31, 2024
https://doi.org/10.13167/2024.29.12

Predicting and evaluating the engineering properties of civic garbage torched bottom ash and sisal fibre-reinforced earth blocks

Abinaya Thennarasan Latha[1] and Balasubramanian Murugesan[2]

[1] School of Architecture and Interior Design, Faculty of Engineering and Technology, SRM Institute of Science and Technology, Kattankulathur, Tamilnadu 603203, India

[2] Department of Civil Engineering, Faculty of Engineering and Technology, SRM Institute of Science and Technology, Kattankulathur, Tamilnadu 603203, India

Corresponding author:
Balasubramanian Murugesan
balasubm1@srmist.edu.in

Received:
July 24, 2024

Revised:
August 24, 2024

Accepted:
September 3, 2024

Published:
December 31, 2024

Citation:
Thennarasan Latha, A.; Murugesan, B.
Predicting and evaluating the engineering properties of civic garbage torched bottom ash and sisal fibre-reinforced earth blocks.
Advances in Civil and Architectural Engineering, 2024, 15 (29), pp. 193-219.
https://doi.org/10.13167/2024.29.12

ADVANCES IN CIVIL AND ARCHITECTURAL ENGINEERING (ISSN 2975-3848)

Faculty of Civil Engineering and Architecture Osijek
Josip Juraj Strossmayer University of Osijek
Vladimira Preloga 3
31000 Osijek
CROATIA

Abstract:
This study examines the impact of civic garbage torched bottom ash (CGTBA), sisal fibre, and cement content on the compressed stabilized earth blocks (CSEB) with respect to their compressive strength and flexural strength. The properties are predicted using artificial neural network (ANN) analysis and response surface methodology (RSM). The study contributes to sustainable construction by emphasizing innovative solutions to reduce waste and improve building materials. The experiment includes four different cement concentrations (6 %, 8 %, 10 %, and 12 %), CGTBA contents (10 %, 20 %, 30 %, and 40 %), and sisal fibre contents (0,25 %, 0,50 %, 0,75 %, and 1,00 %). ANN models predict compressive and flexural strengths with high accuracy (R^2 values: 0,98189 and 0,94951, respectively). Optimization yields a desirability index of 0,724. A detailed comparison between actual and predicted values demonstrates close alignment, validating the ANN-RSM technique's efficacy in estimating responses and identifying influential parameters. Additionally, the ANN-RSM approach optimizes CSEB performance, providing valuable insights into parameter optimization. The use of CSEB stabilized with cement, CGTBA, and sisal fibre has the potential to transform into a sustainable approach to construction materials.

Keywords:
compressed stabilized earth block; compressive strength; flexural strength; artificial neural network; civic garbage torched bottom ash

1 Introduction

Sustainable materials have become increasingly vital in modern construction, reflecting a global shift towards environmentally responsible practices. Among these materials, earthen buildings stand out as one of the earliest and most enduring construction methods, with a history that extends back over 9000 years [1]. Currently, a substantial proportion of the global population lives in buildings constructed of clay materials [2]. Earthen architecture, which includes construction techniques such as cobs, rammed earth, and adobes, represents the diverse heritage of local building practices. These methods depend on organic elements, such as clay, sand, and straw, which are shaped by hand to construct durable and environmentally friendly buildings [3]. Contemporary earthen construction sometimes includes engineering concepts and uses rammed-earth and compressed-earth bricks [4]. Recently, notable progress has been made in compressed stabilised earth block (CSEB) buildings [5]. Traditional earthen construction methods, although sustainable and cost-effective, often face limitations such as low tensile strength and reduced durability, particularly under high humidity conditions. To address these challenges, modern advancements have introduced the use of chemical stabilisers in soil, followed by compression, to create CSEBs. These advancements have been well documented, positioning CSEBs as a promising alternative to conventional materials such as red clay bricks and concrete blocks [6]. CSEBs are increasingly recognised as a feasible contemporary construction method for low-rise structures, primarily because of their environmentally friendly and cost-effective nature [7]. However, CSEBs face several limitations, including relatively low tensile strength, which has been reported to be around 0,1-0,2 MPa [8]. They also exhibit brittle behaviour under stress, leading to cracking and failure [9]. Additionally, their durability is compromised under high-humidity conditions, with increased moisture absorption, leading to reduced performance over time [10]. Recent research has sought to address these limitations by optimising the stabilisers and improving the mix design to enhance the overall performance of CSEBs [11]. These limitations can be overcome by adding the correct quantity of the appropriate stabiliser. Many studies have examined the possibilities of using lime, gypsum, cement, and natural and synthetic fibres [12].

The amount of residential garbage generated in metropolitan areas is growing annually owing to ongoing population growth. Statistics show that almost two billion tons of civic garbage were produced worldwide in 2016. It is projected that with the present pace of increase, 3,4 billion tons of civic garbage will be produced by 2050 [13]. Incineration is currently the most efficient method of handling civic garbage. Garbage can be incinerated to decrease volume by approximately 90 % (or 70 % by mass). This process allows a significant quantity of energy that may be utilised to generate electricity to be recovered and the composition of municipal garbage is altered [14]. Although incineration may significantly decrease the waste volume, specific residues are still created throughout the process. These residues had a 10-20 % fly ash content and an 80-90 % bottom ash concentration. Garbage torched bottom ash (CGTBA) is classified as general garbage and is generated in large volumes [15]. Currently, landfill disposal is the predominant approach for managing CGTBA. After recycling, CGTBA is widely used in the building sector [11]. Some researchers have suggested that CGTBA can be used as an alternative to cement and raw cement materials.

Tripura and Singh et al. explored cement-stabilised rammed-earth bricks ranging in cement concentrations from 0-10 %. Using blocks stabilised with 10 % cement resulted in a maximum compressive strength of 6 MPa [16]. Reddy et al. found that the compressive strength of cement-stabilized rammed earth, with a cement content of 7-10 %, ranged from 4,96-8,44 MPa [17]. According to studies by Walker et al. on cement-stabilised blocks, only 5-10 % cement is required to achieve the desired characteristic strength of 1-3 MPa [18]. Jayasinghe et al. found that rammed-earth walls could be strengthened by adding cement. The addition of 10% cement to sandy soil resulted in the highest strength, measuring 3,71 MPa. The wet-to-dry compressive strength ratios ranged from 0,45-0,60. Cement stabilisation improves the strength and durability of soil [19]. To address the abovementioned limitations and improve seismic resilience, soil has been strengthened by incorporating natural or synthetic fibres. The practice of enhancing soil strength using fibrous elements, such as straw, for the production of mud bricks and walls can be traced back to ancient civilisations [20]. However, it is worth noting that there are currently no universally accepted standardized guidelines for this technique. The size and percentage of reinforcing fibres are among several variables that affect fibre performance [21].

Numerous natural fibres, such as banana, coconut, palm, jute, and barley have been utilised in various amounts, as shown in Table 1 [22]. Bouhicha et al. tested composite soils reinforced with 0-3,5 % barley straw at 10-20; 20-40; and 40-60 mm lengths. The addition to the soil of 1,5 % fibre, with a size ranging from 20 to 40 mm, resulted in a 10-20 % increase in compressive strength when compared to the sample without any fibre reinforcement. However, the fibre length did not significantly influence the observed effects [23]. Danso et al. examined the effects of different aspect ratios of bagasse, palm oil, and coconut fibre on blocks of crushed soil. There was an increase in both compressive and tensile strengths with coconut coir fibre 50 mm or larger [24]. Tripura et al. found that adding coconut coir and paddy straw to cob bricks made them stronger. Researchers looked at different percentages of coconut coir and paddy straw by mass of dry soil, from 0-10 %. According to their research, cob bricks with 5 % fibre were the strongest. Furthermore, the blocks demonstrated increased strength when tested with a 0,75 m drop height [25]. Raj et al. evaluated the effect of coconut fibre reinforcement on rammed-earth bricks. The researchers experimented with different quantities of coconut fibre, ranging from 0% to 1.0%, based on dry soil mass [26]. The compressive strength peaked at 10,42 MPa when 0,8 % coir and 10 % cement were combined, whereas the tensile strength was recorded at 0,2 MPa. A failure to address the influence of fibre length and durability on the performance of fibre-reinforced rammed-earth bricks has been reported [27].

Table 1. Table 1. CSEBs using different fibres and stabilisers in earlier research

Ref	**Fibre** (%)	**Stabilizer** (%)	**WCS** (MPa)	**DCS** (MPa)	**Flexural strength** (MPa)	**Tensile strength** (MPa)
[28]	Sugarcane fibre (0; 0,5; 1,0)	Cement (0; 6; 12)	0,92-2,39	1,22-4,48	0,32-1,54	0,29-0,89
[29]	Date palm fibre (0,05; 0,10; 0,15; 0,20)	Lime (8; 10; 12)	4,80-6,40	6,80-7,80	-	0,70-1,30
[30]	Rice straw fibre (0; 2)	Gypsum (9; 12; 15)	1,89-3,87	2,50-3,50	0,26-1,47	-
[31]	Bagasse fibre (0,25-2,00)	Cement (3; 5; 7)	-	5,67-10,34	-	-
[32]	Vetriver straw fibre (0; 0,5; 1; 1,5; 2; 2,5; 3)	-	-	0,85-1,78	0,36-0,98	-
[33]	Banana fibre (0; 0,5;1,0)	Cement (0; 5; 10)	0,45-1,78	3,12-4,65	0,45-1,12	0,60-0,77
[34]	Coconut fibre (0,25-2,00)	Cement (0; 6; 12)	0,89-2,94	3,35-5,67	0,39-1,45	-
[24]	Oil palm fibre (0,25-1,00)	-	-	2,55-3,48	-	0,20-0,40
[35]	Coir fibre (1; 3; 5)	-	1,68-3,62	2,72-7,63	-	0,14-1,20
[36]	Hibiscus cannabinus fibres (0,2-0,8)	Cement (0; 10)	-	1,95-2,90	0,55-1,13	-

*Note: WCS–wet compressive strength, DCS–dry compressive strength

The strengths of CSEBs vary depending on several variables, such as the amount of cement, sand, clay, CGTBA, and fibres used in their construction. It may be difficult to construct effective regression-based models for predicting the block strength owing to the complicated relationships between these factors [37]. Artificial neural networks (ANNs) and response

surface methodology (RSM) have been successfully used in civil engineering to address this issue [38]. Many researchers have used ANNs to predict the efficacy of CSEBs. Gupta et al. created an ANN model that employed cement, sand, coarse aggregate, water, and modulus as input variables to evaluate the compressive strength of concrete at various phases of development. The actual values matched the predictions [39]. Hossain et al. discovered that ANN models predict the 28-day compressive and tensile strengths of concrete mixtures better than regression models [40]. Pazouki et al. used ANN models to estimate the compressive strength of concrete. These models consider various parameters, including cement type, fly ash concentration, water-to-binder ratio, superplasticiser, and fine and coarse aggregates. The ANN models were found to be good approximations of the experimental results [41]. Using data from several concrete mixtures, Khalegi et al. used ANNs as a predictive tool for estimating the 7th day and 28th day compressive strength of specimens. One-, two-, and three-layer neural networks were trained using the backpropagation technique, and their respective performances were compared. To accurately estimate the strength of the concrete mixtures, the best networks were selected for use [42].
This study investigated the use of sisal fibre and CGTBA in the production of CSEBs to address landfill and circular economy management challenges. The incorporation of these materials reduces waste volume, minimises environmental pollution, and conserves landfill space. Waste incineration byproducts are repurposed as valuable construction materials, minimising the extraction of natural resources and reducing environmental impact. This study emphasises the importance of sustainable construction practices as the strength and durability of CSEBs are enhanced, contributing to eco-friendly building solutions. The incorporation of waste materials also supports efforts to reduce the environmental footprint of construction activities, thereby lowering the demand for conventional building materials. The study also exemplifies circular economy principles by closing the loop of waste management and resource utilisation and transforming waste materials into valuable inputs for construction. CGTBA improves the strength and durability of CSEBs through particle packing, chemical composition, enhanced curing mechanisms, and reduced environmental impact. This fills voids, reduces porosity, and enhances particle interlocking, resulting in a more compact and stronger block structure. The extended curing process can lead to higher strength and more durable blocks over time. Sisal fibres are crucial in the construction industry for providing tensile strength and enhancing the structural integrity of CSEBs. Their inherent mechanical properties and reinforcement capabilities make them an effective reinforcement material for CSEBs, reducing cracking and improving the resistance of the blocks to deformation.
The primary objective of this study was to assess the impact of using CGTBA and sisal fibres as reinforcing materials on the strength and durability of CSEBs. Additionally, this study aimed to determine the optimal mixture of these additives to achieve the best performance. To achieve this, a statistical regression model, along with an ANN and RSM, was developed to predict the compressive and flexural strengths of CSEBs. This model incorporates the proportions of sisal fibres, CGTBA, and cement within the mixture. The combined approach of statistical regression, ANN, and RSM provides a robust framework for academics, designers, and construction professionals to evaluate and optimise the strength characteristics of sisal fibre-reinforced earth blocks.

2 Materials and methods

2.1 Soil

The soil used in this study was sourced from the Auroville, Pondicherry, and Union Territories in southern India. The sample was obtained from depths of 2–5 m below the Earth's surface, sun-dried, and then sifted using a 4,75 mm mesh. The soil used in this study had to be reconstituted because naturally available soil did not have an ideal fine-to-coarse ratio. The soil was classified as poorly graded sand with silt (SP-SM), according to Indian Standard IS: 1498-1970. The physical properties of the soil are summarised in Table 2. The soil gradation is shown in Figure 1a. Soil mineralogy was ascertained using X-ray diffraction (XRD) [43-45].

According to the XRD data shown in Figure 2a, the soil is mostly composed of kaolinite, geothite, katoite, and quartz. Figure 3a shows the scanning electron micrographs of the silt-clay sample, which highlight the granular shape of the particles.

Table 2. Physical characteristics of soil employed in this research

Property	Value
soil classification (as per IS: 1498-1970) specific gravity	Poorly-graded sand with silt (SP-SM) 2,62
Grain size properties	
percentage of gravel	0,00 %
percentage of coarse sand	0,11 %
percentage of medium sand	4,68 %
percentage of fine sand	64,72 %
percentage of silt	25,49 %
percentage of clay	5,00 %
effective size, D10	0,06 mm
D30	0,07 mm
D50	0,22 mm
D60	0,28 mm
coefficient of uniformity, Cu	4,67
coefficient of curvature, Cc	0,29
Proctor test	
optimum moisture content	12,77%
maximum dry density	1950 kg/m^3
Atterberg's limit	
liquid limit	55,4
plastic limit	23,2
plasticity index	22,6

Where; D10 denotes grain diameter corresponds to 10 % finer (effective diameter); D30 grain diameter corresponds to 30 % finer; D50 is mean grain size (grain diameter corresponds to 50 % finer); and D60 is grain diameter corresponds to 60 % finer.

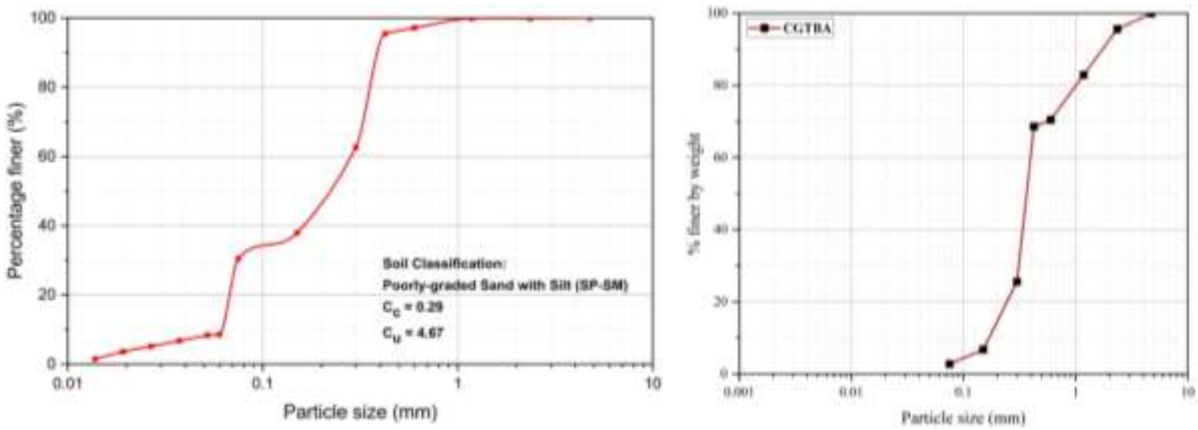

(a) (b)

Figure 1. Grain size distribution: (a) soil and (b) CGTBA

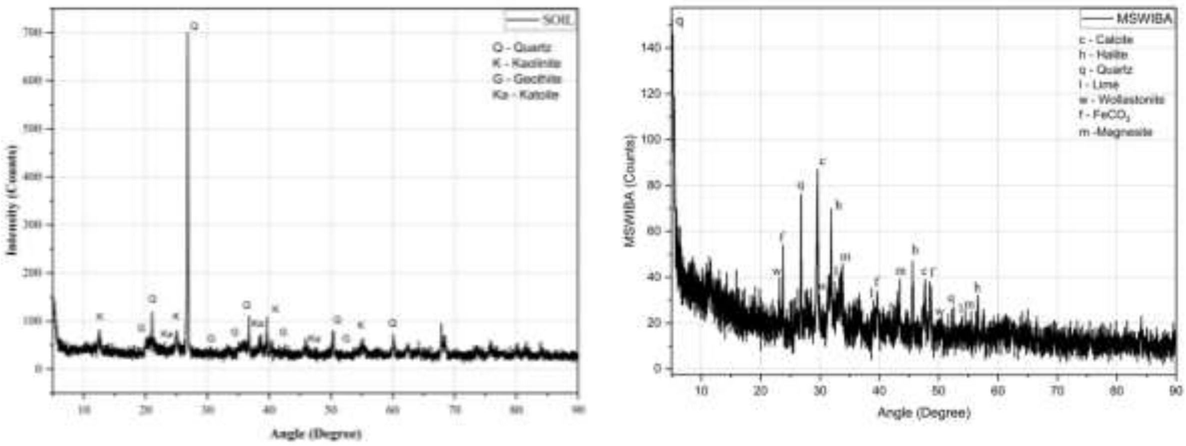

(a) (b)

Figure 2. XRD analysis of raw materials: (a) soil and (b) CGTBA

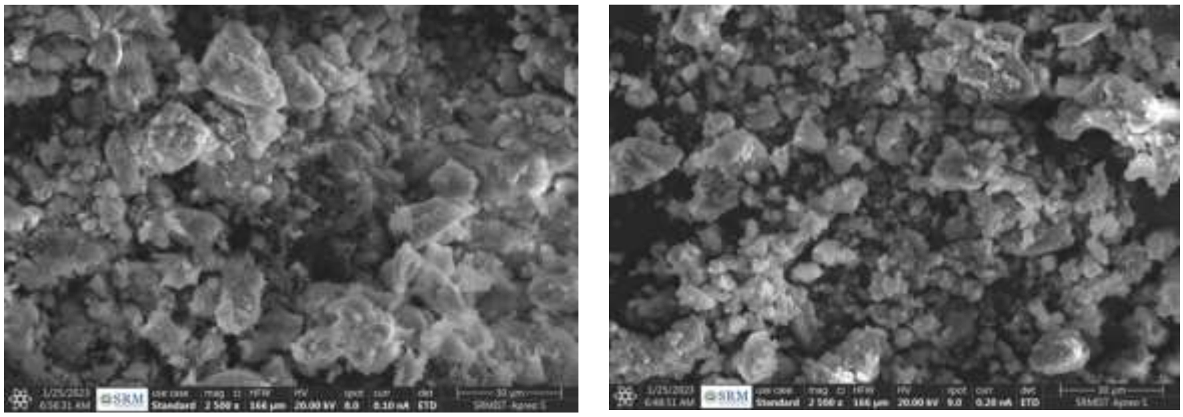

(a) (b)

Figure 3. SEM analysis of raw materials: (a) soil and (b) CGTBA

2.2 Cement

The present investigation used Type I ordinary Portland cement (OPC) of grade 43. The OPC used in the study had a specific gravity of 3,15 and demonstrated an initial setting time of 135 min, followed by a final setting time of 295 min. According to the guidelines outlined in ASTM C109 [46], the compressive strength of the OPC after 28 days of curing was recorded as 47,8 MPa. Table 3 summarises the chemical composition of the cement.

Table 3. Chemical composition of materials (wt %)

Elements	SiO_2	Al_2O_3	Fe_2O_3	CaO	MgO	Na_2O	K_2O	SO_3	TiO_2	MnO	LOI
Soil	45,38	12,12	6,78	19,36	4,66	2,56	1,98	0,56	0,78	0,32	5,50
Cement	22,45	4,13	3,54	62,43	1,62	0,61	0,32	1,36	-	-	3,54
CGTBA	30,75	16,78	7,38	30,29	3,74	2,95	0,99	1,02	2,12	-	3,98

2.3 Civic garbage torched bottom ash

CGTBA was obtained from an incineration facility in Manali, located in the northern part of Chennai (India). At this plant, CGTBA is generated at a rate of 2000 kilograms per day. For the production of CSEBs, air-dried and pulverised CGTBA required to fit through a 4,75 mm screen was employed [12]. Table 3 lists the detailed chemical composition of the CGTBA particles. Table 4 presents the physical characteristics of CGTBA. The bottom ash of Class F status was assigned to the CGTBA particles because its specific gravity was determined to be 2,30. XRD analysis was used to determine the mineral composition. According to the data shown in Figure 2b, the soil and CGTBA were predominantly composed of quartz minerals with a small amount of calcite also being present. The results of the particle size analysis confirm the scanning electron microscopy (SEM) findings shown in Figure 3b that the CGTBA particles are smaller and have more irregular forms than the silt-clay particles.

Table 4. Physical properties of CGTBA

Properties	CGTBA
specific gravity	2,26
water absorption	14,34 %
fineness modulus	2,40
loose bulk density	1125 kg/m^3
compacted bulk density	1326 kg/m^3

2.4 Sisal fibre

Sisal fibre (SF) has numerous advantages over other fibres, such as biodegradability, long lifespan, and minimal maintenance. Fibre with a diameter of 100-300 m that is derived from sisal leaves. SF may be used for various purposes in civil engineering, such as soil stabilisation and plaster panel reinforcement. To enhance the mechanical characteristics and facilitate the development of interlocking mechanisms inside the blocks, the fibres were treated with a sodium hydroxide solution following the guidelines outlined in ASTM D1695 [47]. The SF was immersed in hot water at 70 ± 5 °C for 1 h to remove any surface residues and impurities. The samples were then allowed to air-dry for 48 hours [12]. The SF was subsequently subjected to an alkalization process by immersion in a solution containing 5 % NaOH. Sodium hydroxide pellets were dissolved in distilled water and agitated using a magnetic stirrer to achieve dilution. The untreated SF samples were submerged in NaOH and soaked for 12 h at room temperature. After immersion, the SF was rinsed with distilled water to remove any harmful residual chemicals. The SF was oven-dried for 4 h at 40 °C to eliminate moisture content. NaOH was used to whiten the SF and improve its physical properties, thus strengthening the structural components [48].

The SF preparation process significantly affects the properties and enhances the strength of the CSEB. Initially, hot water treatment removed surface residues such as waxes and gums, which improved the bonding between the SF and the soil matrix, resulting in better interlocking and uniform distribution of SF within the blocks. Following this, the alkalization process with a 5 % NaOH solution further cleaned the SF and modified its surface properties. This treatment increased the surface roughness and improved moisture absorption, leading to stronger adhesion between the SF and the soil matrix. The subsequent drying process ensured that the SF was free of excess moisture, which could otherwise weaken the soil matrix or interfere with curing. Together, these treatments enhanced the mechanical properties of the SF, such as its tensile strength and bonding ability, ultimately contributing to a more robust and durable CSEB. The treated SF improved the load-bearing capacity, reduced the brittleness, and enhanced the resistance of the blocks to environmental conditions, thereby improving the overall performance and longevity of the CSEBs.

2.5 Sample fabrication

The block specimens were produced using a manual single-stroke one-sided compaction machine capable of exerting a pressure range of 2-4 MPa. The CSEBs were prepared using a combination of pulverised dry soil, CGTBA, SF and cement using a power-driven mixer for a minimum duration of 10 min. Subsequently, water was progressively incorporated into the mixture of soil-cement-CGTBA and SFs while continuing the mixing process. To ensure the consistency of the CSEB mix, the dry components were thoroughly mixed in a mechanical mixer before gradually adding water at a controlled speed to ensure an even distribution and prevent segregation. The mixture was monitored visually and manually during the process, with adjustments made as needed to maintain homogeneity. The components were compacted to verify the uniformity in density and moisture content, ensuring consistent quality across all blocks. The optimal moisture content and maximum dry density for the combination of soil-cement-CGTBA and SFs were determined using the standard Proctor test. This test also considered the water requirements of the cement. The dimensions of the conventional block used in this study were 240 × 115 × 90 mm. Following the manufacturing process, the blocks underwent wet and dry curing for 28 days at ambient temperature before further testing [49]. Figure 4 shows a flowchart of block preparation. Various combinations of soil composition and admixtures were utilised, as presented in Table 5, to evaluate the influence of soil gradation on the strength of the blocks and to identify the most suitable admixture for this purpose [50].

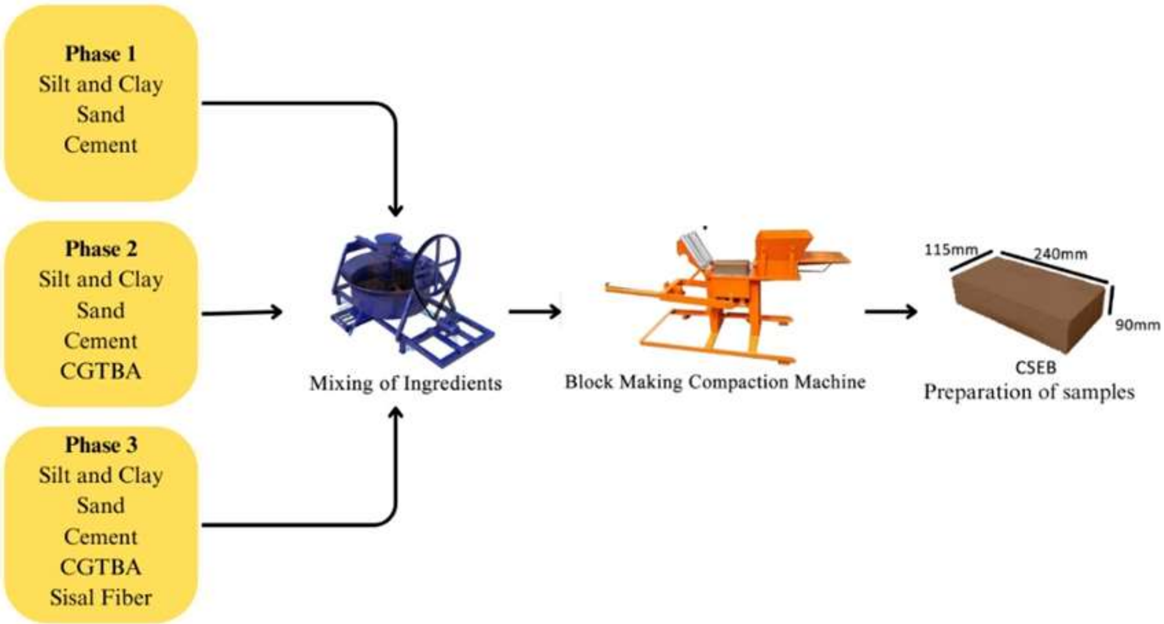

Figure 4. Flow chart of block preparation

Table 5. Combination of materials considered in this study

Series	**Sand** (g)	**Silt & Clay** (g)	**Cement** (g)	**CGTBA** (g)	**Sisal fibre** (g)	**Compressive Strength** (MPa)	**Flexural Strength** (MPa)
CE6	2963	1230	251	0	0	5,55	0,62
CE8	2963	1230	335	0	0	5,97	0,73
CE10	2963	1230	419	0	0	7,79	0,76
CE12	2963	1230	503	0	0	9,07	0,86
M10	2755	1230	419	208	0	7,035	0,77
M20	2547	1230	419	416	0	6,045	0,79
M30	2339	1230	419	624	0	5,435	0,70
M40	2131	1230	419	832	0	5,055	0,57
SF1	2547	1230	419	4,16	6	6,35	0,98
SF2	2547	1230	419	416	12	6,12	1,65
SF3	2547	1230	419	416	18	4,51	1,74
SF4	2547	1230	419	416	24	3,98	1,95

2.6 Experimental test

The compressive strength was assessed using five samples of each mixture, and the flexural strength was assessed using three samples. A compression testing apparatus with a 200-tonne capacity was employed to provide a uniform load until failure occurred [51]. To determine the compressive strength of the CSEB, a method was used that involved applying pressure between two 15 mm-thick steel plates, as shown in Figure 5a. This method uses the failure load and sectional area of a block to calculate its compressive strength [16]. Additionally, a three-point flexural test, as shown in Figure 5b, was performed following the guidelines of the HB 195 standards to evaluate the flexural strength of the CSEB. The blocks were tested using a universal testing machine (UTM) with a maximum capacity of 400 kN. The machine applied a steady force of 2,5 kN per minute until the blocks failed [52].

(a) (b)

Figure 5. Mechanical test setup: (a) compression test and (b) flexural test

2.7 Artificial neural network

An ANN is a set of computational structures inspired by the structure and functionality of the human mind and nervous system. They are widely employed in machine learning and pattern recognition tasks. The activating coefficients, input weights, output neurons, and neural networks all come together to form neurons [53]. Finding the best architecture for a neural network requires optimising the input composition and hidden layer count for both single-layer and multi-layer networks. The units for the inputs, single-weight layer, and outputs comprise a single-layer network [54]. A multi-layer network consists of three layers: input, hidden, and output. Data are received by input neurons, processed by hidden neurons using prejudices and weights, and sent by output neurons via hidden output layer connections [55]. Neural networks are widely used in engineering because of their pattern identification, adaptive learning, autonomy, and real-time operation [56]. An ANN establishes a connection between the input and output parameters by implicit adaptation based on predefined training patterns, distinguishing it from other soft computing methods. In addition, ANN does not place boundaries on the distribution variables that can be handed out. ANNs were chosen for this study because of their ability to model complex non-linear relationships between input variables and outputs, which is particularly beneficial for predicting the mechanical properties of materials such as CSEBs. Traditional regression models often assume a linear relationship, which may not adequately capture the intricate interactions between components such as CGTBA, SFs, and cement in CSEBs. In contrast, an ANN excels in handling non-linearity and can learn from the data to identify patterns and relationships that might be missed by other techniques. The ANN can manage large datasets and automatically adjust to the nuances of the data, thereby improving prediction accuracy.

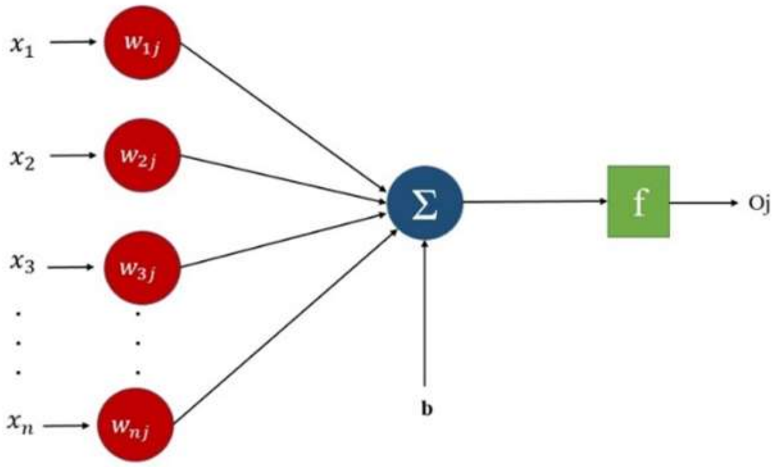

Figure 6. Customary architecture of an ANN

Figure 6 shows the architecture of the ANN; in the given notation, symbol O_j represents the output of the j^{th} neuron, ω_{ij} denotes the weight associated with the j^{th} neuron's input xi, b indicates the bias term, and f denotes the activation function employed by the neuron. A significant number of ANNs use activation algorithms such as the sigmoid, tanh, SoftMax, linear, and Gaussian algorithms. All layers in the network architecture, except for the input phase, utilise these features. Sigmoid algorithms are often used to simulate multi-layer receptive models. The use of backpropagation training was deemed appropriate for addressing the engineering issues encountered in this study.

2.8 Input and output parameters

This research intended to investigate the mechanical characteristics of CSEBs, with a special focus on their significance as a major factor in determining their strength. The next stage in the construction of ANNs is the identification of the input elements that have a substantial impact on the output variables. The input parameters for the experimental observations were the proportions of sand, silt, clay, cement, CGTBA, and SFs, as shown in Figure 7. The selection of these input parameters was driven by both theoretical understanding and empirical evidence from prior studies, which demonstrated their significant roles in determining the compressive and flexural strengths of CSEBs. Cement acts as a stabiliser, enhancing the strength and durability of the block, whereas CGTBA, as a waste-derived material, contributes to sustainability and potentially affects the density and strength of the block. SFs, known for their tensile strength, were used to improve the flexural performance of the blocks. The output parameters, that is, the compressive and flexural strengths, were chosen because they are the primary indicators of the structural integrity and performance of CSEBs in construction applications. These metrics are critical for assessing the suitability of blocks for load-bearing and non-load-bearing purposes. The predicted output parameters were the compressive and flexural strengths, which were evaluated for different mix proportions of the bricks. All datasets included the input parameters and their results. The numbers of input, hidden, and output layers were 5, 10, and 2, respectively, as shown in Figure 8. Although neural network training is vital for success, large amounts of data are required for training, validation, and testing. The neural network (ANN) model had input, hidden, and output layers. The number of neurons in each layer was determined through empirical testing and neural network design standards. To balance the model complexity and performance, testing and cross-validation defined the hidden layer neuron numbers. The number of neurons in the hidden layers was selected to optimise the ability of the model to learn intricate patterns without overfitting. The activation function used in the hidden layers is the rectified linear unit (ReLU), which is used to mitigate the vanishing gradient problem and accelerate model convergence by adding non-linearity.

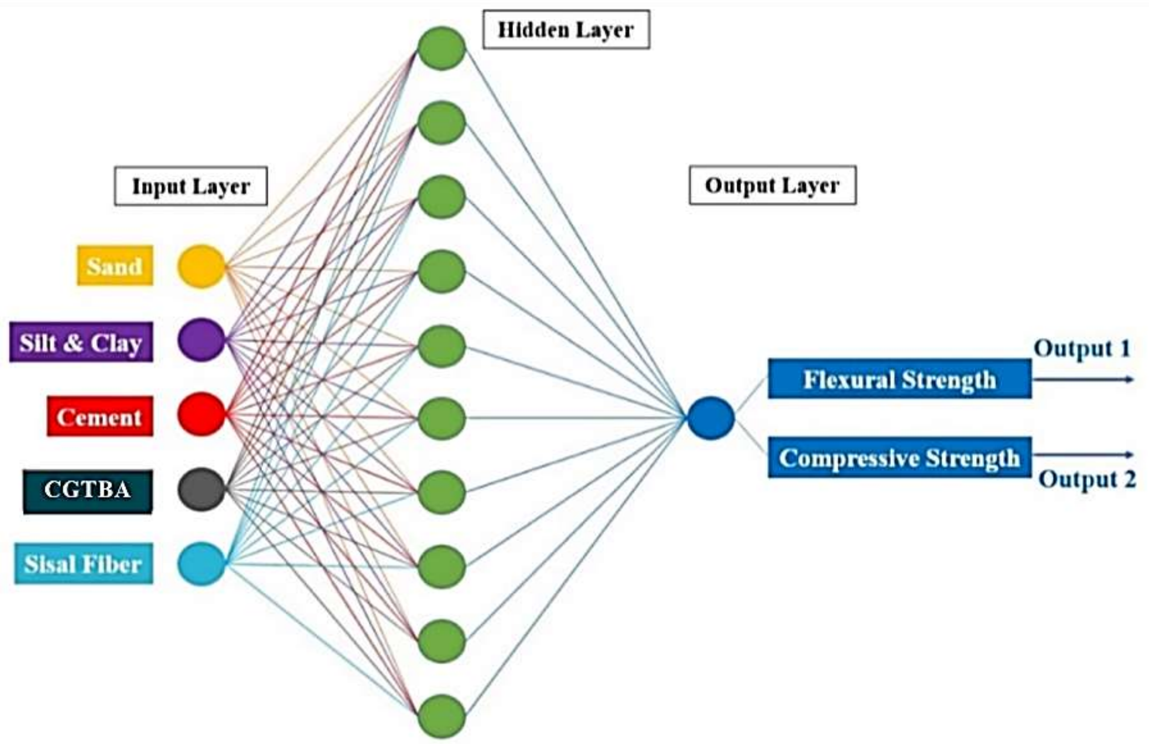

Figure 7. ANN architecture of CGTBA compressed stabilized earth block

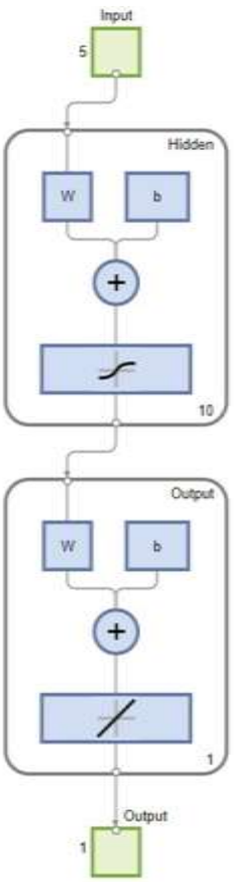

Figure 8. MATLAB representation of the ANN framework

3 Discussion of ANN findings

3.1 Compressive strength

The field-measured compressive strengths of CGTBA blocks were evaluated to validate the precision of the ANN model. Figure 9 shows the neuronal outputs and resulting values of the training, validation, and test datasets in ANN regression plots. In an optimal situation, the data would exhibit clustering patterns that align with the line representing the neural network's outputs that match the anticipated outcomes. The R values for the problem demonstrated a significant correlation across the dataset, with training at 0,99824, validation at 1, testing at 1, and all at 0,98189. Figure 10 illustrates the decline in the mean squared error (MSE) of the approach, which aligns with the anticipated outcome of a well-trained ANN. As shown in the image, the observed trend indicates the effectiveness of framework learning in decreasing epochs, especially in epoch 3. The figure shows three distinct lines, because the input and target vectors were randomly split into three groups. A potential reduction in overfitting may be accomplished by halting the training procedure after the desired degree of performance on the training set is attained. In this specific case, the performance of the validation set surpassed that of the training set, suggesting optimal fitting and obviating the necessity for regularisation.

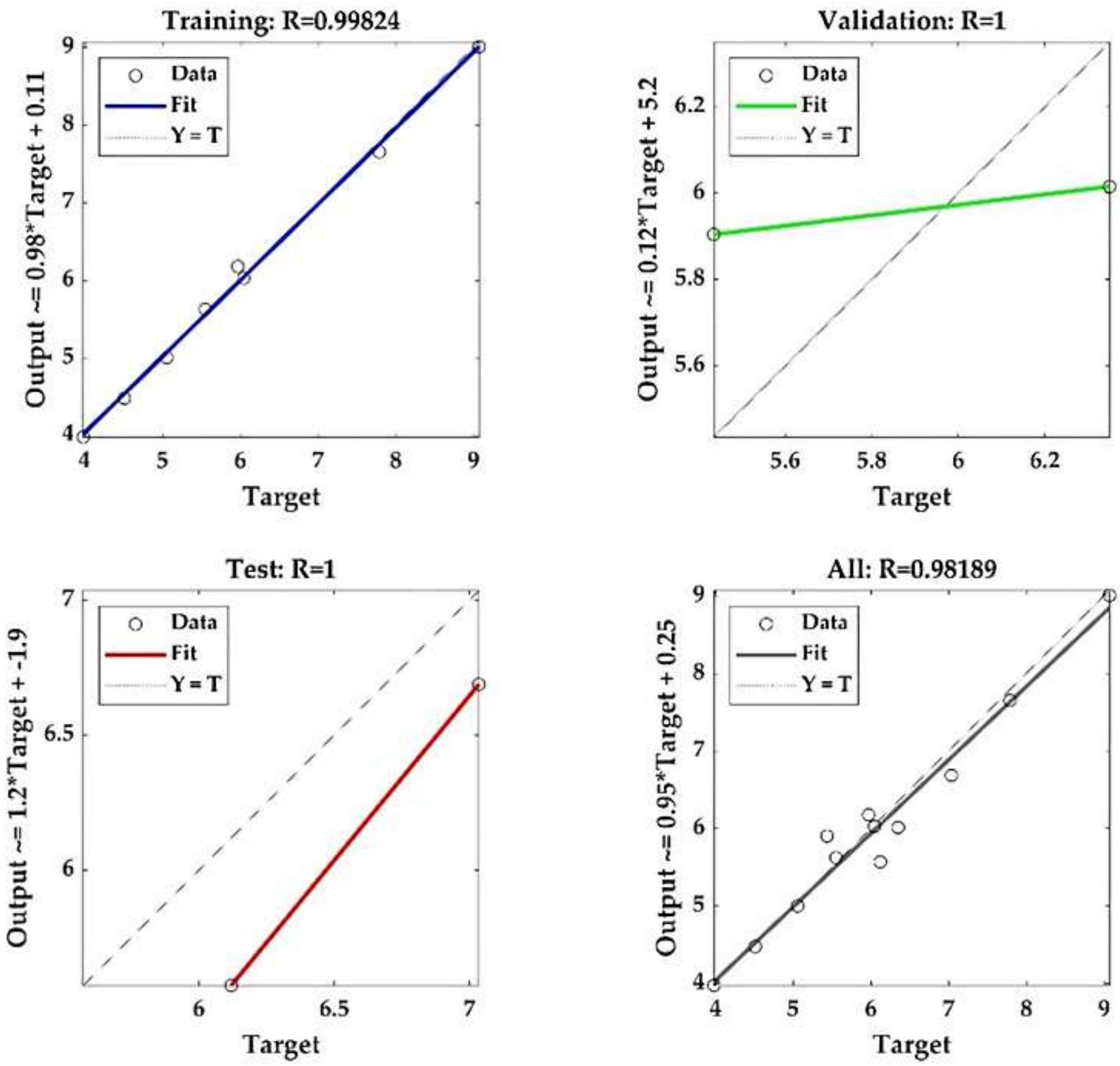

Figure 9. Compressive strength ANN regression illustrations

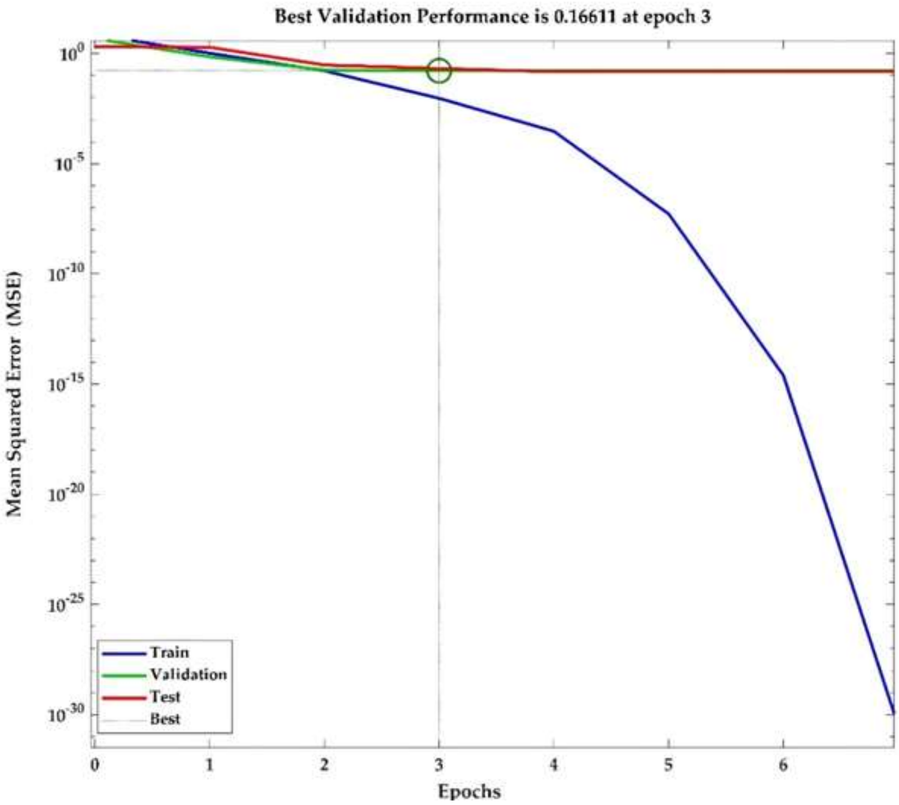

Figure 10. Compressive strength performance graphs

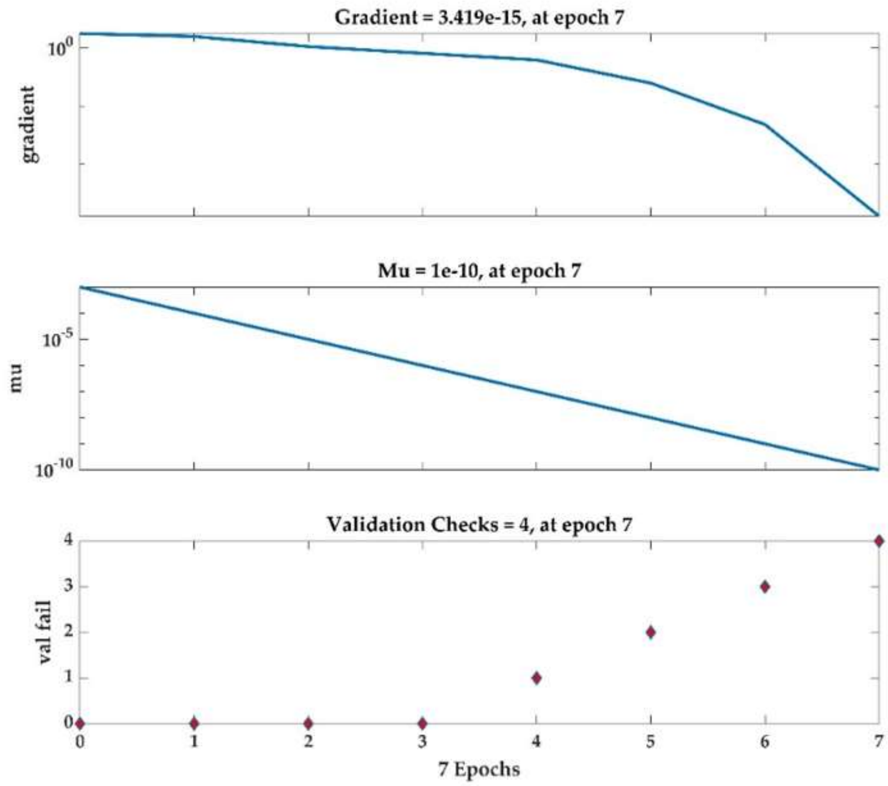

Figure 11. Compression strength data fitting plot

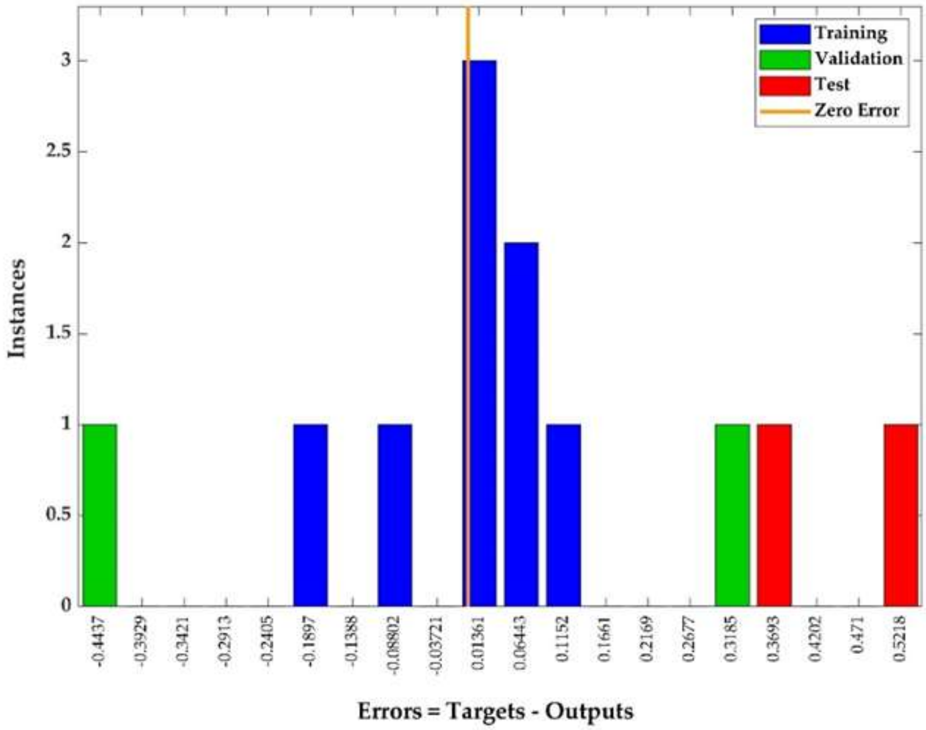

Figure 12. Histogram plot compressive strength

The findings are depicted in Figure 11, which highlights that the strength appears to reach a stable state after epoch 3. This observation demonstrates a noteworthy linkage with the model parameters. The fit plot indicates that the predicted values should be close to the diagonal line, reflecting a high degree of predictive accuracy. Figure 12 displays histograms of the errors in the neural network training, validation, and testing. The graph illustrates that the error rates for the data fitting were evenly distributed around zero. The graph displays a histogram of the errors during the training, validation, and testing phases. Owing to the limited number of bins available, the error margins are becoming increasingly narrow. A higher cement content generally led to increased compressive strength up to the optimal point. Beyond this point, the marginal gains diminished, suggesting an optimal cement content of approximately 10 % for maximizing strength. The incorporation of CGTBA enhanced compressive strength up to 30 %. This suggests that CGTBA can effectively replace traditional aggregates without compromising their strength, thus contributing to sustainable waste management. SF improved compressive strength at moderate levels (0,75 %), likely owing to its reinforcing properties. However, an excessive fibre content can lead to diminishing returns or negative effects owing to potential fibre clumping.

3.2 Flexural strength

Flexural strength was determined experimentally, and the collected data were subsequently utilised to validate the ANN model. The network findings for the training, validation, and assessment sets are presented, along with the appropriate result values, in Figure 13. To achieve an optimal fit, the data must comply with the line that correlates the precise alignment of the neural network outputs with the predicted outcomes [57]. With training at 0,989, validation at 1, testing at 1, and all at 0,94951, all datasets have a proficient fit.

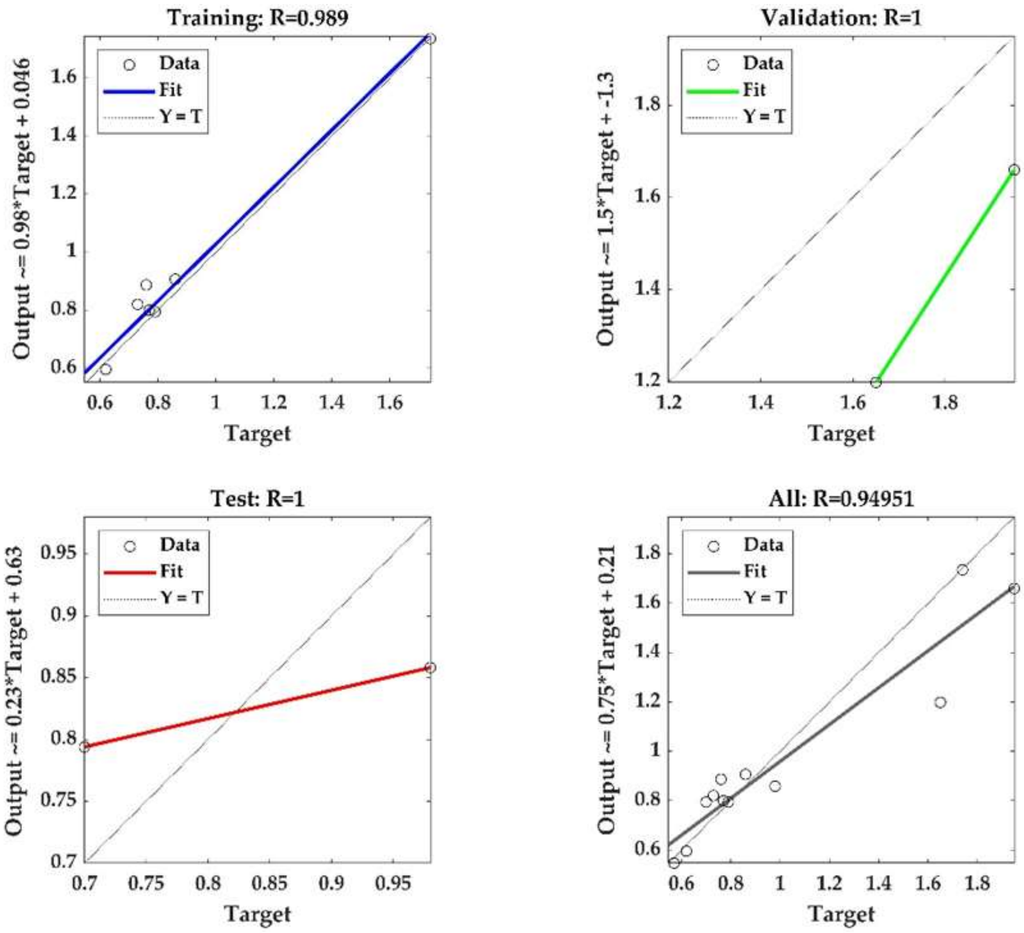

Figure 13. ANN flexural strength regression graphs

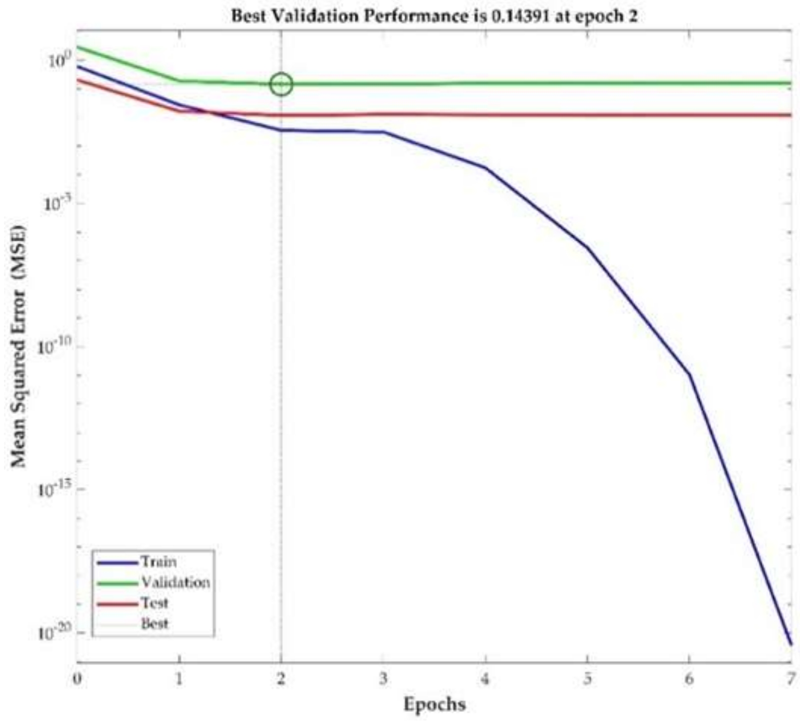

Figure 14. Flexural strength performance plot

Figure 14 illustrates the MSE of the network, which exhibits a decreasing trend, as expected for a proficiently trained ANN. The declining trend observed in the graph further indicates the efficacy of network learning during epoch 2 [58]. The existence of the three distinct traces in the given figure is due to the stochastic partitioning of the input and desired vectors into three distinct groups. The occurrence of overfitting can be restricted by promptly halting the training process once the target performance level is attained on the training dataset. In this scenario, it is evident that the validation performance surpasses the training performance, indicating a superior fit without the necessity for regularisation. The regression plots show a near-linear relationship between the predicted and actual values, where most of the data points align closely with the 45-degree line. The low MSE value of 00094 indicates that the average squared difference between the predicted and actual values is minimal, reflecting the ability of the model to make precise predictions with little deviation from the actual measurements. The data points in the regression plots do not show significant deviations or outliers, suggesting that the model performed consistently well across the entire dataset.

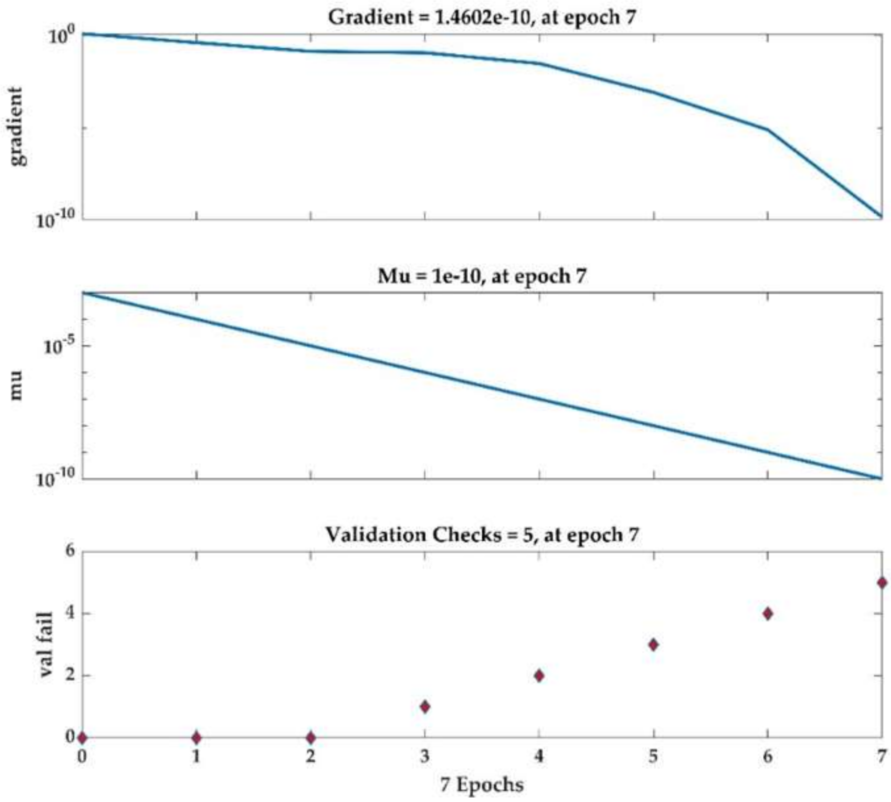

Figure 15. Flexural strength fit charts

The neural network training, validation, and testing error histograms are shown in Figure 16. The data fitting error rates are linear around 0, as shown in the graph. There were 20 bins in the error histogram for the training, validation, and testing data. According to the histogram, the error margins are more compact. Figure 15 shows that the strength increases after seven epochs, which is consistent with this hypothesis. The fit plots show that the anticipated values follow a diagonal line, which is an instance of prediction.

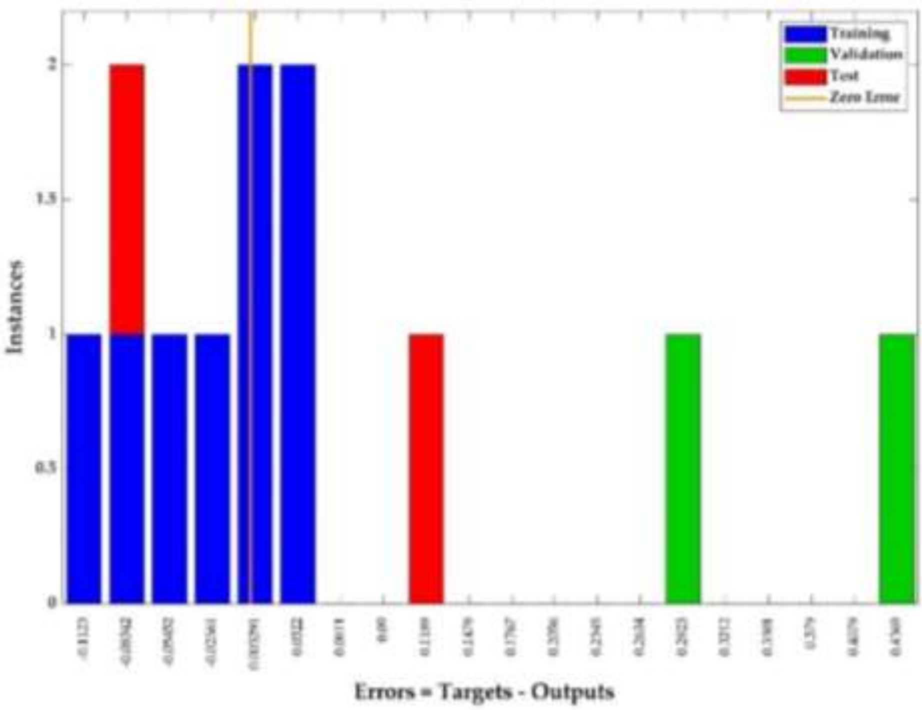

Figure 16. Flexural strength histogram plot

A feedforward neural network (FNN) with backpropagation training was chosen for its ability to model complex non-linear relationships between the input parameters and output properties of compressed stabilised earth blocks. Adam optimisation further enhanced the training process, providing robust and reliable performance. The FNN was trained using the training dataset, and hyperparameters such as the number of hidden layers, neurons per layer, learning rate, and batch size were optimised through cross-validation. The model performance was validated using a validation dataset. High R^2 values (0,98189 for the compressive strength and 0,94951 for the flexural strength) indicated the accuracy and reliability of the model. The MSE values for the ANN model were 0.0094 for the compressive strength and 0,0036 for the flexural strength. The MSE measures the average squared difference between the predicted and actual values, with lower values indicating higher prediction accuracy. In this study, the low MSE values demonstrate that the predictions of the ANN model are very close to the actual measured values, confirming its high precision and reliability. The high R^2 values and low MSE values validate the effectiveness of the ANN model in predicting the mechanical properties of the CSEBs.

3.3 Impact of CGTBA and SF on the properties of CSEBs

3.3.1 Mechanisms and effects of change in compressive strength

These findings suggest that the inclusion of CGTBA in the cement led to an initial improvement in strength at various cement concentrations. This improvement reached its maximum at a certain CGTBA content, which was regarded as the optimum level. The enhanced strength achieved by including CGTBA up to a suitable concentration was attributed to the pozzolanic reactions occurring between CGTBA and calcium hydroxide (CH) generated during the cement hydration process. The reaction between cement and soil results in the formation of calcium silicate hydrate (C–S–H), which fills the pores and enhances strength. Consequently, a C–S–H gel was formed, which enhanced the mixture and increased the internal connectivity of the soil structure. This led to an improvement in the CGTBA content from 10-40 %, resulting in a gradual reduction in compressive strength from 5,05-7,03 MPa during dry testing. When the CGTBA content is increased, the compressive strength initially improved at a cement concentration of 10 %. However, after attaining the optimum CGTBA concentration, the strength began to decrease. Calcium hydroxide, a byproduct of cement crystallisation, reacts with the added CGTBA to form calcium aluminate silicate. This component hardens the mixture and increases the internal cohesion of the soil matrix. In the absence of cement in the structure, the reaction required for significant strength gain does not occur. Furthermore, when an appropriate amount of CGTBA is added to the mixture, it has a unique capacity to interact with the hydrated byproduct of cement crystallisation. Excessive addition of CGTBA to the required amount of cement resulted in the presence of unreacted CGTBA particles in the mix. This prevents the formation of a strong interconnecting link between the soil particles, resulting in a reduction in the strength of the stabilised earth blocks. The lower panel represents 1 % SF and 20 % CGTBA. A greater proportion indicated that the SF content was 0,25 % and the CGTBA content was 20 %. The compression strengths of SF-reinforced blocks with 0.25%, 0.50%, 0.75%, and 1 % fibre content, 20 % CGTBA, and stabilised with 10% cement content were 3,00 %, 3,97 %, 7,81 %, and 10,23 % lower than the blocks without fibres. The addition of SF to CSEBs makes buildings more flexible and therefore more resistant to earthquakes. CSEBs that have been strengthened with SF show many small cracks and a slow failure process, with the fibres filling in new cracks as they appear. In contrast, unreinforced CSEBs undergo abrupt and complete failure, typically forming a single long and wide crack. Thus, fibre reinforcement improves post-peak performance by effectively redistributing loads across cracks. The traditional building blocks include mud, adobe, fired clay and compressed earth. The compressive strengths of these materials are as follows: mud blocks (1-5 MPa); adobe blocks (2-3 MPa); fired clay bricks (3-5 MPa); and compressed earth blocks (4-5 MPa). The compressive strength of CSEB with CGTBA and SF, in contrast, is 5,0-7,5 MPa, outperforming these conventional blocks. The manufacturing of CSEB is limited by the requirement for appropriate soil. An overview of the strength qualities of CSEBs improved by several stabilisers, as documented in earlier studies, is presented in Tables 1 and 6. The tables list many stabilising strategies and how each affects the mechanical properties of CSEBs.

3.3.2 Mechanisms and effects of change in flexural strength

Under three-point compression, all the blocks that were fractured were separated into two parts. With the inclusion of CGTBA, the flexural strength increased to a maximum of 20 % replacement of sand quantity, with a maximum strength of 0,79 MPa. This may be attributed to the pore-filling ability of CGTBA, which results in a reduction in fracture propagation. In addition, the flexural strength decreased when the CGTBA content exceeded 20%, ultimately reaching a minimum of 0,57 MPa.

Table 6. Comparison of the strength of CSEBs with various stabilizers

Reference	**Stabilizer (Content)**	**Block Size** (mm)	**Compressive strength** (MPa)	**Flexural strength** (MPa)
[4]	Fly ash (0-30 %) + Cement (0-10 %)	245 × 127 × 76	2,11-7,11	0,18-1,35
[16]	Crushed brick waste (6-24 %) + Cement 10 %	290 × 140 × 100	3,69-9,57	0,89-2,65
[59]	Recycled aggregate (15 %) + cement (0-8 %)	145 × 140 × 90	2,40-5,40	0,25-1,19
[60]	Waste rice ash (0-20 %) + cement (4-8 %)	241 × 114 × 70	2,14-7,00	0,80-2,96
[61]	GBFS (0-45 %) + Cement (6-12 %)	305 × 143 × 105	1,05-1,55	-
[62]	Saw dust ash (0-10 %) + Cement (4-10 %)	190 × 90 × 90	2,49-5,85	-
[63]	Construction waste (5-20 %) + cement (6-10 %)	350 × 100 × 175	2,50-8,00	-
[64]	Lime (2-8%) + Cement (0-6%)	230 × 108 × 75	-	0,32-1,54

The blocks containing SF had a higher flexural strength than the CGTBA samples, which was consistent with the findings of the compressive strength tests. The SF4 sample exhibited a maximum strength of 1,95 MPa. The flexural strength increased compared with that of the CG20 mix. The isotropic matrix generated by the SF enhanced bonding, resulting in increased flexural strength. SF in the reinforced blocks effectively reduced the propagation of microcracks as the load increased. This behaviour demonstrates greater ductility, which can be attributed to the use of SF. Furthermore, all mixes of the CSEB specimens satisfied the strength requirements of the standards.

3.4 Response surface analysis of compressive and flexural strength

RSM was used as part of the data analysis in this study to assess and model the responses. During the early phases of the process, the independent variables were sand, silt, clay, cement, CGTBA, and SF in the CSEB. Mechanical parameters, such as compressive strength and flexural strength, were chosen as the responses of interest. Experimental runs were performed using the central composite design (CCD) technique to obtain empirical data on responses after 28 days. This information was collected directly from the experimental runs, allowing a thorough examination of the correlations between the dependent and independent variables (mechanical characteristics).

3.5 ANOVA results

The analysis of variance (ANOVA) outcomes is presented in Table 7, employing RSM for the compressive and flexural strengths, demonstrated a high level of significance, as indicated by the p-values being less than 0.0001 for the two variables. This suggests that the models exhibit statistical significance and can be used to generate predictions. The F-values exhibited a significant range from 0,69-2,89, further substantiating the statistical significance of the model [65]. The p-value was less than 0,0001, which indicates a high degree of proximity and a strong level of fit and predictive capacity within the model. In general, the findings of this study confirm that the RSM models utilised for compressive and flexural strengths are highly reliable in their predictions. Consequently, these models can be considered reliable tools for optimising the strength of CSEBs [66]. The high statistical significance and low standard deviations indicate that the independent variables significantly influence the mechanical properties of the CSEBs, with the compressive strength model showing particularly strong predictive power.

Table 7. The ANOVA outcomes

Response	Standard deviation	Mean	Df	Mean Square	F-value	p-value
CS	1,67	5,67	5	0,3966	2,89	< 0,0001
FS	0,37	0,96	10	1,8200	0,69	< 0,0001

An optimisation process was performed to determine the ideal values of the independent variables that would yield the highest possible degree of the desired outcome. The study was conducted by defining the objectives for the aspects, including input parameters and output, under various conditions and degrees of significance to achieve the desired target function. The desirability value, frequently recognised as the optimisation result outcome, falls within an acceptable range of 0-1 (or 0-100 %). The high F-values and low p-values for both models indicate that the predictors used (cement, CGTBA, and SF content) significantly affect the compressive and flexural strengths of the CSEBs. An F-value of 2,89 suggests that the model explains more variance than would be expected by chance, indicating that the model is statistically significant for compressive strength. The F-value for flexural strength was lower at 0,69. This suggests that the model explains some variance in flexural strength but is less effective than the compressive strength model. A p-value of less than 0,0001 indicates a high level of statistical significance, indicating that the model's predictions for the compressive and flexural strengths are reliable and not due to random chance.

3.6 Model diagnostics plot

Graphs comparing the predicted and actual values of the compressive and flexural strengths are presented in Figures 17 and 18 respectively. These figures facilitate the assessment of the precision of the model and illustrate the correlation between the experimental data and predictions. The validity and accuracy of the models were verified by aligning the data points along a 45-degree line of fit, which signified the optimal path representing the predicted and actual responses.

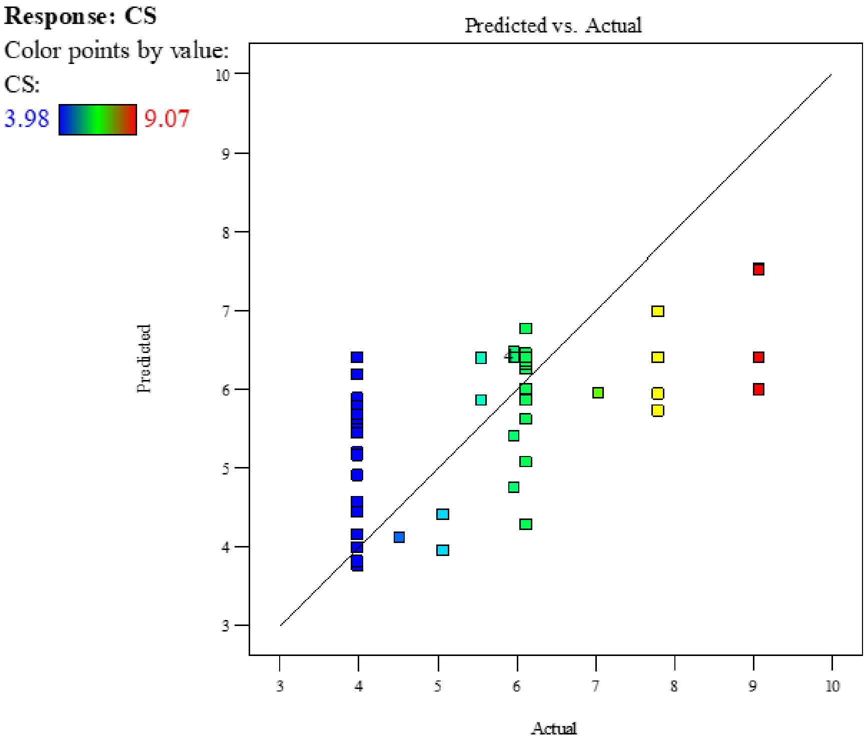

Figure 17. Actual vs. predicted graph for compressive strength

Table 8. The goals and outcomes of optimization results

Factors		Input Factors					Responses (Output Factors)	
		Sand (g)	**Silt & Clay** (g)	**Cement** (g)	**CGTBA** (g)	**Sisal Fibre** (g)	**CS** (MPa)	**FS** (MPa)
Value	Minimum	2131	1230	251	0	0	3,98	0,57
	Maximum	2963	1250	503	832	24	9,07	1,95
Goal		in range	in range	minimize	maximize	maximize	maximize	maximize
Optimization Result		2963	1237	251	832	24	6.31	1.67
Desirability			0,724 (72,4 %)					

This validation confirms the reliability of the model in optimising the CSEB compositions, enabling precise adjustments to the material ratios for improved structural performance. The scatter plot underscores the effectiveness of the ANN model in capturing the underlying data patterns, thereby ensuring robust predictions.

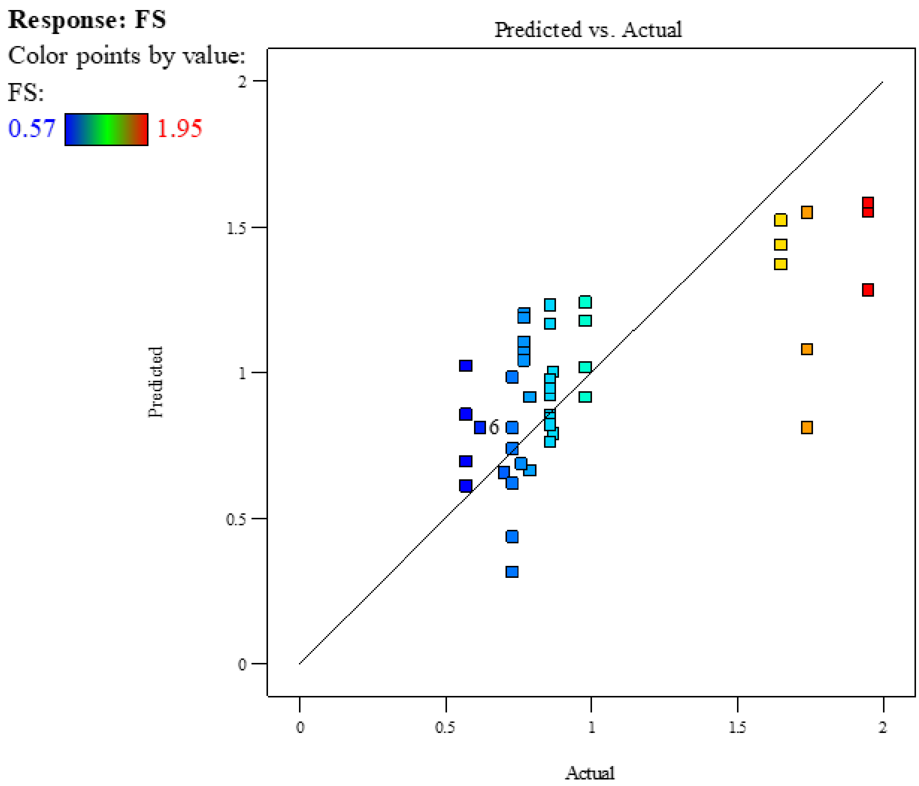

Figure 18. Actual vs. predicted graph for flexural strength

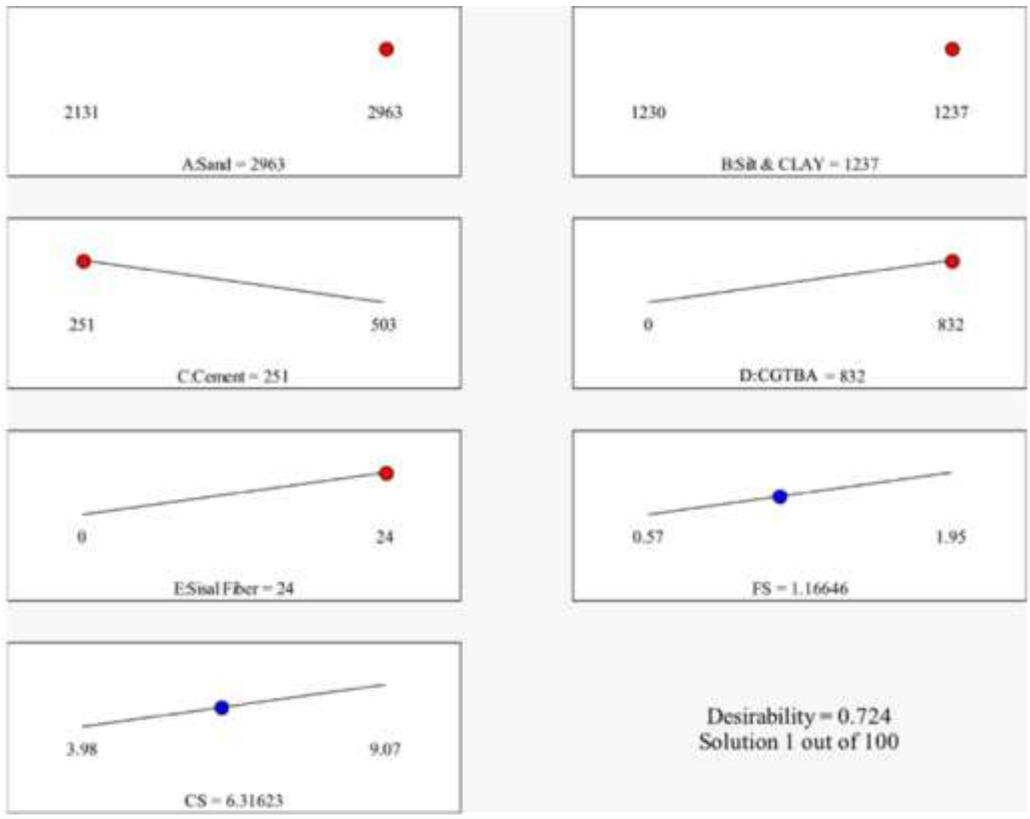

Figure 19. Optimization ramp for compressive and flexural strength

A higher proximity to the numerical value of 1 indicates an ideal result. Table 8 presents the objectives and criteria for the optimisation of the present scenario. Based on the selected criteria and degree of significance, the table illustrates the optimal combination of the system input variables and intended responses. Given the multitude of factors involved in the experiment and the extensive range of potential outcomes derived from the numerical analysis, the results are quite promising. The results of the optimization indicated that the highest values of the compressive and flexural strengths of 6,31 MPa and 1,67 MPa could be achieved for the brick by combining 2963, 1237, 251, 832 and 24 grams of sand, silt and clay, cement, CGTBA, and SF respectively, which is depicted in Table 5 and Figure 19. The degree of proximity between the suggested approach and actual outcome determines the desirability criteria. For optimal results, the aim is to achieve a desirability identical to 1. A desirability score of 0,724, shown in Figure 20, indicates that response optimisation was attainable for all input factors which influences the compressive and flexural strength.

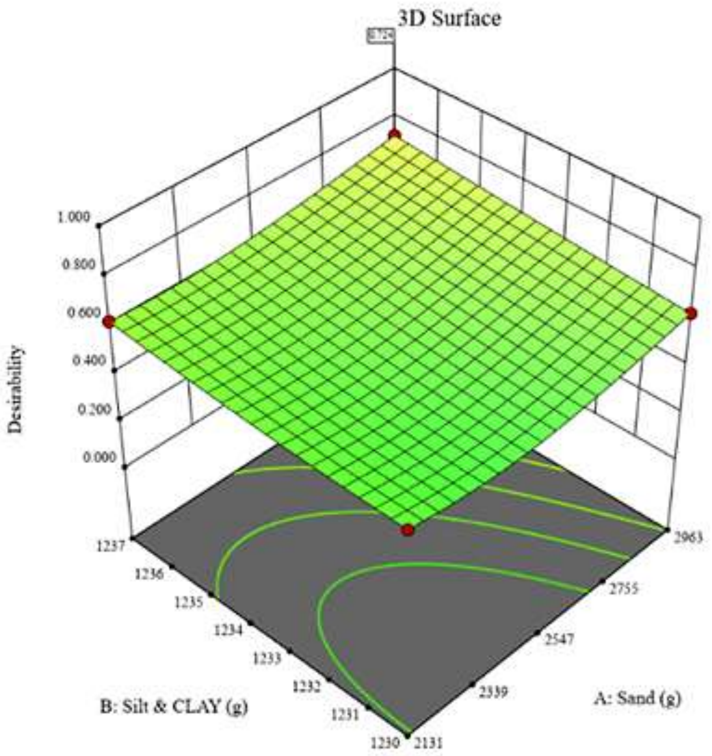

Figure 20. Desirability of the optimization

4 Conclusions

This paper discusses the implementation of an ANN model to assess the compressive and flexural strengths of CSEB with CGTBA and SF.

- In this study, the CSEB was used, with CGTBA substituted for a fraction of the sand component. The use of a composition consisting of 20 % CGTBA, 10 % cement, and 1 % SF has been shown to provide optimal and statistically significant outcomes.
- A novel hybrid model combining an ANN and optimisation techniques was developed to determine the optimum strength of the CSEB. Based on the empirical results derived from the developed model, it can be inferred that the ANN model is potentially effective for forecasting both compressive and flexural strengths.
- The ANN model exhibited satisfactory performance in terms of compressive and flexural strengths, with R^2 values of 0,98189 and 0,94951 respectively. The results

indicate its ability to predict the strength of the blocks, as supported by the obtained and researched data.

- The MSE values for the compressive and flexural strength tests were 0,0094 and 0,0036, respectively. These minimal values indicate a strong correlation between the test findings.
- The models provided in this study aim to guide designers and practising engineers in predicting the optimum compressive and flexural strengths of compressed stabilised earth blocks commonly used in building applications.
- The model generated from the R^2 analysis indicates slight disparities between the observed and projected values.
- Based on the ANOVA results, the R^2 values had a difference of less than 0,2, which indicates that the model requires further validation.
- The optimisation results indicate a desirability value of 0,724 for the compressive and flexural strengths, which is satisfactory and applicable for further prediction.

In recent years, there has been growing interest in earthen buildings owing to their economic, social, and environmental sustainability. The primary limitation of soil is its inadequate strength. The results of this study indicate that it is possible to create strong and durable CSEBs using an appropriate mix of CGTBA and SF. Future research could explore the use of alternative natural fibres, such as flax, jute, or coconut coir, to further enhance the mechanical properties of CSEBs. Additionally, investigating the combined use of different stabilisers such as lime, fly ash, and rice husk ash could optimise the strength and durability of the blocks. Long-term studies on the effects of environmental factors such as moisture and temperature fluctuations would also provide valuable insights for the practical application of these materials in various climates.

References

[1] Bahar, R.; Benazzoug, M.; Kenai, S. Performance of compacted cement-stabilised soil. *Cement and Concrete Composites*, 2004, 26 (7), pp. 811-820. https://doi.org/10.1016/j.cemconcomp.2004.01.003

[2] Alene, T. E.; Mohammed, T. A.; Gualu, A. G. Use of sisal fiber and cement to improve load bearing capacity of mud blocks. *Materials Today Communications*, 2022, 33, 104557. https://doi.org/10.1016/j.mtcomm.2022.104557

[3] Kondekar, V. G.; Jaiswal, O. R.; Gupta, L. M. Ultrasonic Pulse Velocity Testing of Gadhi Soil Adobe Bricks. *International Journal of Engineering Research in Mechanical and Civil Engineering (IJERMCE)*, 2018, 3 (1), pp. 2456-1290.

[4] Islam, M. S.; Elahi, T. I.; Shahriar, A. R.; Mumtaz, N. Effectiveness of fly ash and cement for compressed stabilized earth block construction. *Construction and Building Materials*, 2020, 255, 119392. https://doi.org/10.1016/j.conbuildmat.2020.119392

[5] Bachar, M.; Azzouz, L.; Rabehi, M.; Mezghiche, B. Characterization of a stabilized earth concrete and the effect of incorporation of aggregates of cork on its thermo-mechanical properties: Experimental study and modelling. *Construction and Building Materials*, 2015, 74, pp. 259-267. https://doi.org/10.1016/j.conbuildmat.2014.09.106

[6] Iwaro J.; Mwasha, A. Effects of Using Coconut Fiber-Insulated Masonry Walls to Achieve Energy Efficiency and Thermal Comfort in Residential Dwellings. *Journal of Architectural Engineering*, 2019, 25 (1). https://doi.org/10.1061/(ASCE)AE.1943-5568.0000341

[7] Elahi, T. E. et al. Suitability of fly ash and cement for fabrication of compressed stabilized earth blocks. *Construction and Building Materials*, 2020, 263, 120935. https://doi.org/10.1016/j.conbuildmat.2020.120935

[8] Walker, P.; Stace, T. Properties of some cement stabilised compressed earth blocks and mortars. *Materials and Structures*, 1997, 30 (9), pp. 545-551. https://doi.org/10.1007/BF02486398

[9] Jaquin, P. 12 - History of earth building techniques. In: *Woodhead Publishing Series in Energy, Modern Earth Buildings*, Hall, M. R.; Lindsay, R.; Krayenhoff, M. (eds.). Woodhead Publishing Limited; 2012, pp. 307-323. https://doi.org/10.1533/9780857096166.3.307

[10] Kebaili, N.; Kehila, Y.; Bensalem, R. Role of perceived ecological quality in a scale for measuring attitude toward earthen building techniques; some findings from a survey on compressed stabilized earth blocks in Auroville, India. *Journal of Asian Architecture and Building Engineering*, 2024, 23 (3), pp. 933-960. https://doi.org/10.1080/13467581.2023.2257282

[11] Abinaya, T. L.; Balasubramanian, M. A circular economy in waste management carrying out experimental evaluation of compressed stabilized earth block using municipal solid waste incinerator fly ash. *Journal of Engineering Research*, 2022, 10. https://doi.org/10.36909/jer.ACMM.16319

[12] Thennarasan Latha, A.; Murugesan, B.; Skariah Thomas, B. Compressed earth block reinforced with sisal fiber and stabilized with cement: Manual compaction procedure and influence of addition on mechanical properties. *Materials Today: Proceedings*, 2023. https://doi.org/10.1016/j.matpr.2023.04.373

[13] Chen, D. M. The world's growing municipal solid waste: trends and impacts. *Environmental Research Letters*, 2020, 15 (7), 074021. https://doi.org/10.1088/1748-9326/ab8659

[14] Marieta, C.; Guerrero, A.; Leon, I. Municipal solid waste incineration fly ash to produce eco-friendly binders for sustainable building construction. *Waste Management*, 2021, 120, pp. 114-124. https://doi.org/10.1016/j.wasman.2020.11.034

[15] Li, Z. et al. Research on the durability and Sustainability of an artificial lightweight aggregate concrete made from municipal solid waste incinerator bottom ash (MSWIBA). *Construction and Building Materials*, 2023, 365, 129993. https://doi.org/10.1016/j.conbuildmat.2022.129993

[16] Kasinikota, P.; Tripura, D. D. Evaluation of compressed stabilized earth block properties using crushed brick waste. *Construction and Building Materials*, 2021, 280, 122520. https://doi.org/10.1016/j.conbuildmat.2021.122520

[17] Venkatarama Reddy. B. V.; Jagadish, K. S. Embodied energy of common and alternative building materials and technologies. *Energy and Buildings*, 2003, 35 (2), pp. 129-137. https://doi.org/10.1016/S0378-7788(01)00141-4

[18] Morel, J. C.; Mesbah, A.; Oggero, M.; Walker, P. Building houses with local materials: means to drastically reduce the environmental impact of construction. *Building and Environment*, 2001, 36 (10), pp. 1119-1126. https://doi.org/10.1016/S0360-1323(00)00054-8

[19] Jayasinghe, C.; Kamaladasa, N. Compressive strength characteristics of cement stabilized rammed earth walls. *Construction and Building Materials*, 2007, 21 (11), pp. 1971-1976. https://doi.org/10.1016/j.conbuildmat.2006.05.049

[20] Turco, C.; Junior, A. C. P.; Teixeira, E. R.; Mateus, R. Optimisation of Compressed Earth Blocks (CEBs) using natural origin materials: A systematic literature review," *Construction and Building Materials*, 2021, 309, 125140. https://doi.org/10.1016/j.conbuildmat.2021.125140

[21] Iwaro J.; Mwasha, A. Effects of Using Coconut Fiber-Insulated Masonry Walls to Achieve Energy Efficiency and Thermal Comfort in Residential Dwellings. *Journal of Architectural Engineering*, 2019, 25 (1). https://doi.org/10.1061/(ASCE)AE.1943-5568.0000341

[22] Subramanian, G. K. M.; Balasubramanian, M.; Jeya Kumar, A. A. A Review on the Mechanical Properties of Natural Fiber Reinforced Compressed Earth Blocks. *Journal of Natural Fibers*, 2022, 19 (14), pp. 7687-7701. https://doi.org/10.1080/15440478.2021.1958405

[23] Bouhicha, M.; Aouissi, F.; Kenai, S. Performance of composite soil reinforced with barley straw. *Cement and Concrete Composites*, 2005, 27 (5), pp. 617-621. https://doi.org/10.1016/j.cemconcomp.2004.09.013

[24] Danso, H. Improving Water Resistance of Compressed Earth Blocks Enhanced with Different Natural Fibres. *The Open Construction and Building Technology Journal*, 2017, 11 (1), pp. 433-440. http://dx.doi.org/10.2174/1874836801711010433

[25] Kasinikota, P.; Tripura, D. D. Evaluation of compressed stabilized earth block properties using crushed brick waste. *Construction and Building Materials*, 2021, 280, 122520. https://doi.org/10.1016/j.conbuildmat.2021.122520

[26] Imjai, T. et al. Deflections of high-content recycled aggregate concrete beams reinforced with GFRP bars and steel fibres. *Engineering Structures*, 2024, 312, 118247. https://doi.org/10.1016/j.engstruct.2024.118247

[27] Raj, S.; Mohammad, S.; Das, R.; Saha, S. Coconut fibre reinforced cement stabilized rammed earth blocks. *World Journal of Engineering*, 2017, 14 (3), pp. 208-216. https://doi.org/10.1108/WJE-10-2016-0101

[28] Kumar N.; Barbato, M. Effects of sugarcane bagasse fibers on the properties of compressed and stabilized earth blocks. *Construction and Building Materials*, 2022, 315, 125552. https://doi.org/10.1016/j.conbuildmat.2021.125552

[29] Taallah B.; Guettala, A. The mechanical and physical properties of compressed earth block stabilized with lime and filled with untreated and alkali-treated date palm fibers. *Construction and Building Materials*, 2016, 104, pp. 52-62. https://doi.org/10.1016/j.conbuildmat.2015.12.007

[30] Akinyemi, B. A.; Mami, O.; Adewumi, J. R. Utilisation of treated rice straw waste fibre as reinforcement in gypsum – cement unfired clay bricks. *Innovative Infrastructure Solutions*, 2022, 7, 308. https://doi.org/10.1007/s41062-022-00911-y

[31] Alavéz-Ramírez, R.et. al. The use of sugarcane bagasse ash and lime to improve the durability and mechanical properties of compacted soil blocks. *Construction and Building Materials*, 2012, 34, pp. 296-305. https://doi.org/10.1016/j.conbuildmat.2012.02.072

[32] Paul, S.; Islam, M. S.; Hossain, M. I. Suitability of Vetiver straw fibers in improving the engineering characteristics of compressed earth blocks. *Construction and Building Materials*, 2023, 409, 134224. https://doi.org/10.1016/j.conbuildmat.2023.134224

[33] Thanushan K.; Sathiparan, N. Mechanical performance and durability of banana fibre and coconut coir reinforced cement stabilized soil blocks. *Materialia*, 2022, 21, 101309. https://doi.org/10.1016/j.mtla.2021.101309

[34] Thanushan, K. et al. Strength and Durability Characteristics of Coconut Fibre Reinforced Earth Cement Blocks. *Journal of Natural Fibers*, 2021, 18 (6), pp. 773-788. https://doi.org/10.1080/15440478.2019.1652220

[35] Sreekumar, M. G.; Nair, D. G. Stabilized Lateritic Blocks Reinforced With Fibrous Coir Wastes. *International Journal of Sustainable Construction Engineering and Technology*, 2013, 4 (2), pp. 23-32.

[36] Millogo, Y.; Morel, J. C.; Aubert, J. E.; Ghavami, K. Experimental analysis of Pressed Adobe Blocks reinforced with Hibiscus cannabinus fibers. *Construction and Building Materials*, 2014, 52, pp. 71-78. https://doi.org/10.1016/j.conbuildmat.2013.10.094

[37] Paul, S.; Islam, M. S.; Elahi, T. E. Potential of waste rice husk ash and cement in making compressed stabilized earth blocks: Strength, durability and life cycle assessment. *Journal of Building Engineering*, 2023, 73, 106727. https://doi.org/10.1016/j.jobe.2023.106727

[38] Sridhar, R.; Imjai, T.; Laory, I. Experimental and Numerical Investigation of Hybrid Fiber Reinforced Concrete for Vibration-Based Damage Assessment. *Engineered Science*, 2024, 30, 1174. http://dx.doi.org/10.30919/es1174

[39] Gupta, T. et al. Prediction of mechanical properties of rubberised concrete exposed to elevated temperature using ANN. *Measurement*, 2019, 147, 106870. https://doi.org/10.1016/j.measurement.2019.106870

[40] Hossain, K. M. A.; Anwar, M. S.; Samani, S. G. Regression and artificial neural network models for strength properties of engineered cementitious composites. *Neural Computing and Applications*, 2018, 29, pp. 631-645. https://doi.org/10.1007/s00521-016-2602-3

[41] Pazouki, G.; Golafshani, E. M.; Behnood, A. Predicting the compressive strength of self-compacting concrete containing Class F fly ash using metaheuristic radial basis function neural network. *Structural Concrete*, 2021, 23 (2), pp. 1191-1213. https://doi.org/10.1002/suco.202000047

[42] Al-Gburi, M.; Yusuf, S. A. Investigation of the effect of mineral additives on concrete strength using ANN. *Asian Journal of Civil Engineering*, 2022, 23, pp. 405-414. https://doi.org/10.1007/s42107-022-00431-1

[43] Bureau of Indian Standards. IS: 2720 (Part 4 - 1985). *Methods of Test for Soils, Part 4: Grain Size Analysis*. New Delhi, India: IS; 1985.

[44] Bureau of Indian Standards. IS:2720-7. *Methods of test for soils, determination of water content dry density relation using light compaction*. New Delhi, India: IS; 1980.

[45] Bureau of Indian Standards. IS: 2720 (part 5):1985. Determination of Liquid limit and Plastic limit of soil. New Delhi, India: IS; 1985.

[46] ASTM International. ASTM C109/C109M-02. Standard Test Method for Compressive Strength of Hydraulic Cement Mortars. USA: ASTM; 2020.

[47] iTeh Standards. C. Derivatives. iTeh Standards. 07, 2023.

[48] Thennarasan Latha, A.; Murugesan, B. Compressed stabilised earth block synergistically valorising municipal solid waste incinerator bottom ash and sisal fiber: Strength, durability and life cycle analysis. *Construction and Building Materials*, 2024, 441, 137514. https://doi.org/10.1016/j.conbuildmat.2024.137514

[49] Sridhar, R. et al. Influence of Nanoparticles and PVA Fibers on Concrete and Mortar on Microstructural and Durability Properties. *Fibers*, 12 (7), 54. https://doi.org/10.3390/fib12070054

[50] Thennarasan Latha, A.; Murugesan, B.; Thomas, B. S. Compressed Stabilized Earth Block Incorporating Municipal Solid Waste Incinerator Bottom Ash as a Partial Replacement for Fine Aggregates. *Buildings*, 2023, 13 (5), 1114. https://doi.org/10.3390/buildings13051114

[51] Thennarasan Latha, A.; Murugesan, B.; Kabeer, K. I. S. A. Valorisation of municipal solid waste incinerator bottom ash for the production of compressed stabilised earth blocks. *Construction and Building Materials*, 2024, 423, 135827. https://doi.org/10.1016/j.conbuildmat.2024.135827

[52] Elahi, T. E.; Shahriar, A. R.; Alam, M. K.; Abedin, M. Z. Effectiveness of saw dust ash and cement for fabrication of compressed stabilized earth blocks. *Construction and Building Materials*, 2020, 259, 120568. https://doi.org/10.1016/j.conbuildmat.2020.120568

[53] Fausett, L. V. *Fundamentals of Neural Networks - Architectures, Algorithms, and Applications*. India: Pearson Education; 2006.

[54] Basheer, I. A.; Hajmeer, M. Artificial neural networks: fundamentals, computing, design, and application. *Journal of Microbiological Methods*, 2000, 43 (1), pp. 3-31. https://doi.org/10.1016/S0167-7012(00)00201-3

[55] Rogers, J. L. Simulating Structural Analysis with Neural Network. *Journal of Computing in Civil Engineering*, 1994, 8 (2). https://doi.org/10.1061/(ASCE)0887-3801(1994)8:2(252)

[56] Armaghani, D. A. et al. Development of hybrid intelligent models for predicting TBM penetration rate in hard rock condition. *Tunnelling and Underground Space Technology*, 2017, 63, pp. 29-43. https://doi.org/10.1016/j.tust.2016.12.009

[57] Hashmi, A. F.; Bilal, M. A. A.; Baqi, M. S. A. GA - based hybrid ANN optimization approach for the prediction of compressive strength of high - volume fly ash concrete mixes. *Asian Journal of Civil Engineering*, 2022, 24, pp. 1115-1128. https://doi.org/10.1007/s42107-022-00557-2

[58] Ahmed, A. H. A.; Jin, W.; Ali, M. A. H. Artificial Intelligence Models for Predicting Mechanical Properties of Recycled Aggregate Concrete (RAC): Critical Review. *Journal of Advanced Concrete Technology*, 2022, 20 (6), pp. 404-429. https://doi.org/10.3151/jact.20.404

[59] Bogas, J. A.; Silva, M.; Glória Gomes, M. Unstabilized and stabilized compressed earth blocks with partial incorporation of recycled aggregates. *International Journal of Architectural Heritage*, 2019, 13 (4), pp. 569-584. https://doi.org/10.1080/15583058.2018.1442891

[60] Paul, S.; Islam, M. S.; Elahi, T. E. Potential of waste rice husk ash and cement in making compressed stabilized earth blocks: Strength, durability and life cycle assessment. *Journal of Building Engineering*, 2023, 73, 106727. https://doi.org/10.1016/j.jobe.2023.106727

[61] Sekhar, D. C.; Nayak, S. Utilization of granulated blast furnace slag and cement in the manufacture of compressed stabilized earth blocks. *Construction and Building Materials*, 2018, 166, pp. 531-536. https://doi.org/10.1016/j.conbuildmat.2018.01.125

[62] Elahi, T. E.; Rafat, A.; Alam, K.; Abedin, Z. Effectiveness of saw dust ash and cement for fabrication of compressed stabilized earth blocks. *Construction and Building Materials*, 2020, 259, 120568. https://doi.org/10.1016/j.conbuildmat.2020.120568

[63] Malkanthi, S. N.; Wickramasinghe, W. G. S.; Perera, A. A. D. A. J. Use of construction waste to modify soil grading for compressed stabilized earth blocks (CSEB) production. *Case Studies in Construction Materials*, 2021, 15, e00717. https://doi.org/10.1016/j.cscm.2021.e00717

[64] Nagaraj, H. B.; Rajesh, A.; Sravan, M. V. Influence of soil gradation, proportion and combination of admixtures on the properties and durability of CSEBs. *Construction and Building Materials*, 2016, 110, pp. 135-144. https://doi.org/10.1016/j.conbuildmat.2016.02.023

[65] Anderson, M. J.; Whitcomb, P. J.; Kraber, S. L.; Adams, W. *Handbook for Experimenters*. USA: Stat-Ease; 2017.

[66] Abdulkadir, I. et al. Effect of Graphene Oxide and Crumb Rubber on the Drying Shrinkage Behavior of Engineered Cementitious Composite (ECC): Experimental Study, RSM---Based Modelling and Optimization. In: *Sustainable Practices and Innovations in Civil Engineering*, Naganathan, S.; Mustapha, K. N.; Palanisamy, T. (eds.). Singapore: Springer, 2021. https://doi.org/10.1007/978-981-16-5041-3_3